Distribution of Chemoattractants in a Heterogeneous Tissue and its Impact on Cell Cluster Migration

REU Site: Interdisciplinary Program in High Performance Computing
Jessica Cooley[1], Aaron George[2], Zachary Mekus[3], Victoria Sabo[4]
Graduate assistant: Morgan Strzegowski[1]
Faculty mentor: Bradford E. Peercy[1]
Client: Michelle Starz-Gaiano[5]

[1]Department of Mathematics and Statistics, UMBC
[2]Department of Mathematics, University of Maryland College Park
[3]Department of Computer Science and Engineering, Washington University in St. Louis
[4]Department of Mathematics and Statistics, Georgetown University
[5]Department of Biological Sciences, UMBC

August 11, 2017

Abstract

Cell migration is the process in living organisms by which the body heals and diseases spread, so comprehension of this mechanism is beneficial to understanding its applications. We studied the cluster cell migration in the egg chamber of *Drosophila melanogaster*, or fruit flies, because it is easy to observe and is relatively simple in that organism. A previous model simulates the cell cluster's migration using forces to determine movement of many individual cells [6][7][4]. We improved and revised this system, creating a geometrically accurate model of the egg chamber and mapping the diffusion of the chemoattractants through that domain using a reaction diffusion system. In addition, the base implementation was updated to more accurately simulate the cell migration process. This model aided us in addressing several uncertainties of cluster cell migration, such as identifying the source and quantity of the chemoattractants, the rate at which they are taken in by other cells in the egg chamber, if at all, and the time needed for them to reach the polar and border cells at the anterior of the chamber that gives the most faithful representation of experimental results.

1 Introduction

Cell migration is an essential part of life to many organisms. For example, cell migration is an integral part of human healing. If this process malfunctions, it can cause detrimental results including cleft palate, arthritis, and cancer metastasis, so it is crucial to learn as much as possible about cell movement through research in order to prevent such malfunctions. Studying other organisms and how their cells migrate can lead to a better understanding of the process of cell movement itself. This paper specifically investigates the cell migration in *Drosophila melanogaster* reproduction [7].

2 Background

The process of clustered cell migration is a detailed, multi-step process. The polar cells begin the migration by signaling to the epithelium of the ovary chamber, causing the border cells to surround the polar cells and form a cluster. The border cells are integral to the migration of the polar cells because, although all the cells in the cluster are receiving signals which direct them towards the oocyte, only the border cells are capable of moving and therefore carry the immobile polar cells along with them in the cluster. Due to the feasible range of migratory force observed in the cell cluster migration, there is a defined range of the possible number of border cells involved

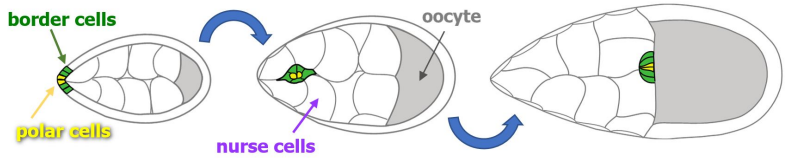

Figure 1: Diagram of Cell Cluster Migrating Through Egg Chamber [5]

in order to result in successful migration [6]. Any number of border cells outside the range of 6 to 10 will result in failure of the polar cell migration to resemble that as seen in-vivo, which is why the cell cluster consists of $6-10$ border cells as well as two polar cells [2]. The border cells are observed to rotate their positions, alternating which border cell is leading the cluster [7]. Once the cluster forms, the receptors Platelet-Derived Growth Factor/Vascular Endothelial Growth Factor (PVR) and Epidermal Growth Factor Receptor(EGFR) guide it in the direction of the oocyte as the cluster navigates through the maze of nurse cells in response to PVF/EGF secretion from the oocyte. [2]. Upon arriving at the oocyte, the cluster of polar and border cells then begins a new migration as part of *Drosophila* oogenesis in the dorsal direction [1] (see Figure 1 for a visual of the start of the cluster cell migration process).

From previous research [2], it was proposed that a chemoattractant distributed uniformly across the egg chamber might be a valid way to initiate the cell movement. However, Duchek et al. suggests that this is not the case, as they experimentally witnessed that a uniform distribution of the guidance chemoattractant actually impeded the cell migration [2]. In our research, because of Duchek, we were motivated to verify that a uniform distribution of chemoattractant would not result in accurate cluster migration. We did this by secreting the chemoattractant from the entire epithelium and oocyte surface. It resulted in unsuccessful cell cluster migration (please see section 4.3 for more details).

Previous models of cell migration assume that the migratory force is proportional to the component of the concentration gradient perpendicular to the axis of interaction between two adjacent cells [7]. They also assumed that the gradient is always constant. This paper involves developing a more accurate model of the spread of chemoattractants throughout the egg chamber using a standard three-dimensional diffusion equation with a linear uptake term at the nurse cells.

3 Methodology

3.1 The Geometry of the Domain

In previous work, a model was created in which the border and polar cells migrated to the oocyte in the egg chamber of fruit flies [7]. The model simulates the egg chamber using Identical Math Cells (IMCs), with each part of the chamber being composed of one or more IMCs. Although this model was sufficient in showing parts of the clustered cell migration, it only displayed the polar and border cells moving in response to a constant gradient.

In our new model, we simulated the diffusion and used the calculated gradient to improve the accuracy of the previous model. To obtain the geometry of the domain of diffusion, we imported the IMCs from the previous model, and generated the convex hull of the center of the IMCs representing the exterior of the egg chamber (the border, polar, and epithelial cells, as well as the oocyte). Then for each nurse cell, we generated an alpha shape containing the centers of the IMCs, and used the volume formed by the outer edges of these boundaries as the geometry to calculate the diffusion (Figure 2). In this model, the egg chamber is approximately a paraboloid of length $409.5\,\mu m$ ending in the oocyte, a circle of radius $146.25\,\mu m$, and centered around $y = z = 146.25\,\mu m$. We realize that this may be larger than reality, but the results are still relevant.

3.2 Diffusion of Chemoattractants

Unlike previous models which assumed a constant gradient, our model calculates gradients for the diffusion process across the egg chamber[2]. We calculate the diffusion of chemoattractants over our updated geometry. It is understood that the chemoattractants originate from a source at the

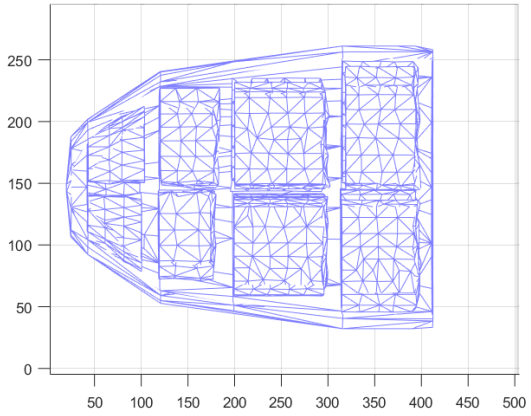

Figure 2: Geometry of Egg Chamber (µm)

Variable	Units
D	$\mu m^2\, s^{-1}$
k	s^{-1}
σ	$pM\, \mu m\, s^{-1}$
φ	$\mu m\, s^{-1}$

Table 1: Units of Variables
pM (picoMolar) is $1 \times 10^{-12}\, mol\, L^{-1}$

oocyte and diffuse anteriorly across the egg chamber. This then triggers the departure of the polar and border cell cluster from the epithelium and their consequential migration towards the oocyte. [2].

Included below are the equations used in our model of chemoattractant diffusion. The base of our model, equation (1), is the diffusion-reaction equation, which represents the spread of heat through a material or the spread of gas through space, and for our purposes the spread of molecules in the egg chamber. The variable D is the diffusion coefficient, and k represents the rate at which the chemoattractant breaks down in the egg chamber. The boundary conditions, equations (2) through (4), model the behavior of diffusion at the surfaces of the egg chamber. These are Neumann conditions, modeling the derivative of the concentration in the direction normal to the boundary, in this case, the flux. Equation (2) represents the secretion of chemoattractants with parameter σ being the value of the constant source, while equation (3) models the uptake of the chemoattractant which depends on the concentration at the boundary, with parameter ϕ being the rate. Equation (4) indicates that the boundaries at all other points do not let any chemoattractant in or out. The boundary conditions can easily be changed to model secretion or uptake at other boundaries to test different hypotheses. Units of the variables can be found in Table 1.

$$\frac{\partial u}{\partial t} = D\left(\frac{\partial^2 u}{\partial x^2} + \frac{\partial^2 u}{\partial y^2} + \frac{\partial^2 u}{\partial z^2}\right) - ku \tag{1}$$

$$-D\frac{\partial u}{\partial n}\Big|_{\text{boundary source of chemoattractant}} = \sigma \tag{2}$$

$$-D\frac{\partial u}{\partial n}\Big|_{\text{boundary of nurse cells}} = -\phi u \tag{3}$$

$$-D\frac{\partial u}{\partial n}\Big|_{\text{all other boundaries}} = 0 \tag{4}$$

Due to the complex shape and boundary conditions, equation (1) cannot be solved analytically. We instead use the MATLAB Partial Differential Equation Toolbox and function *pdesolve* to numerically solve this equation. This solver implements the finite element method to obtain an approximate solution.

IMCs	α
Polar and border cell	15000
Two polar cells	4000
Two border cells	4000
Two IMCS in the same nurse cell	1.5
Any other pair	1

Table 2: α Values

Constant	Original Value	Updated Value
C_s	$2.1 \times 10^{-14}\,\mathrm{N}$	$1.4 \times 10^{-13}\,\mathrm{N}$
C_r	$5.8 \times 10^{-17}\,\mathrm{N\,\mu m^{-3}}$	$2.3 \times 10^{-16}\,\mathrm{N\,\mu m^{-3}}$
C_a	$6.6 \times 10^{-19}\,\mathrm{N\,\mu m^{-1}}$	$2.6 \times 10^{-18}\,\mathrm{N\,\mu m^{-1}}$
C_m	$4.3 \times 10^{-14}\,\mathrm{N}$	$1.7 \times 10^{-13}\,\mathrm{N}$
C_r from oocyte	$5.8 \times 10^{-17}\,\mathrm{N\,\mu m^{-3}}$	$9.2 \times 10^{-16}\,\mathrm{N\,\mu m^{-3}}$

Table 3: Values of Constants

3.3 Updating the Migration Model

Our original code, written by David Stonko, uses four forces to simulate the polar cells and border cells migrating to the oocyte: stochastic, repulsive, adhesive, and migratory [4][6][7]. The equations for the movement of IMCs and each force are as follows:

$$\begin{aligned}
\frac{dU}{dt} &= \frac{1}{\mu}(F_s + F_r + F_a + F_m) \\
F_s &= C_s * (N(0,1), N(0,1), N(0,1)) \\
F_r &= C_r * (19.5\,\mu\mathrm{m} - ||d||)^3 \frac{d}{||d||} \\
F_a &= C_a * \alpha * (29.25\,\mu\mathrm{m} - ||d||) \frac{d}{||d||} \\
F_m &= C_m * \frac{\nabla u}{||\nabla u||_\perp}
\end{aligned}$$

Where U is the location of an IMC, $\mu = 0.066\,\mathrm{pN\,s\,\mu m^{-1}}$ is the dynamic viscosity of cytoplasm (using the values from water), $N(0,1)$ is a normally distributed random variable with mean 0 and standard deviation 1, d is the displacement vector between two cells, α is a constant depending on the two cells interacting (Table 2), and $\frac{\nabla u}{||\nabla u||_\perp}$ is the component of the normalized gradient perpendicular to the interaction between two cells [6]. The diameter of an IMC is 19.5 µm.

We updated the code which changed the behavior of the simulation. The migratory force acts only between border cells and non-border cells. A border cell pushes off another cell in the direction of the component of the chemoattractant gradient that is perpendicular to the interaction between the cells. This results in a border cells feeling a force towards the oocyte and the other cell feels an equal force in the opposite direction. The simulation that we started with attempted to model this, but the equal and opposite force on the non-border cell was calculated to be zero, despite the specification of the migratory force in the model [7]. In addition, the previous model allowed a border cell to push off another border cell when that should not occur biologically. This resulted in the border cells to unnaturally push off each other without the other feeling any force back. The border cells were consequently able to travel quickly as a pack without pushing off the nurse cells. We updated this by using the correct index (updated constants can be found in Table 3).

Another change in the migratory force calculation is the introduction of the gradient, as described above. The original model made no reference to normalizing the gradient, but still used the gradient in calculating the migratory force [6]. When modeling the diffusion of the chemoattractant, we observed that the magnitude of the gradient varied significantly between the two ends of the egg chamber, therefore we normalized the gradient so that the magnitude of the migratory force would not vary the same way.

We also restructured the migration and plotting code so it could be run in parallel. For each time step, the forces on each cell are calculated independently of the forces on all other cells, which facilitated computing these force calculations in parallel. Similarly, plotting each frame of the animation is independent of all other frames, so the graphics were able to be done in parallel as well. In both cases, we used MATLAB's *parfor* function and ran the code with 1 node and 16 processors on UMBC's High Performance Computing Facility using maya [3].

The original code checked for neighbors (defined as IMCs within two IMC diameters from the cluster) every 40 time steps. This means that instead of looking at every pair of cells to find those close enough to exert a force, it only checks for close cells among a list of neighbors. Then, every 40 time steps the code created a new neighbors list for each cell by checking every cell and adding those that are within a range larger than the maximum force, but small enough that every cell is not included. This was meant to save time. However, it could cause some force interactions not to be calculated because they are outside the neighbor list but still close enough that it should exert a force. With the parallelization of other calculations, we were able to avoid using the neighbor list and simply calculate forces from every potential IMC interaction and remain computationally efficient.

4 Results

4.1 Diffusion Parameters and Their Impact on Spread of Chemoattractant

We analyzed aspects of the diffusion of chemoattractant to understand more fully the cell cluster migration process. Our results arose from a diffusion of 18000 seconds (5 hours). This timespan was chosen because it corresponded with the migration time line of the reproductive cycle of fruit flies. We tested different aspects of the diffusion that might be relevant to researchers. We altered each parameter individually while leaving the rest at their default values: $D = 1\,\mu m^2\,s^{-1}$, $k = 1 \times 10^{-4}\,s^{-1}$, $\phi = 0\,\mu m\,s^{-1}$, $\sigma = 100\,pM\,\mu m\,s^{-1}$, $h_{max} = 100$. In our tests, unless otherwise stated, the chemoattractant secretes from the epithelium where the x-value is greater than $\geq 300\,\mu m$.The chemoattractant also secretes from the face of the oocyte, located at x-value $409\,\mu m$. Given that these default choices are somewhat arbitrary, we changed the parameter values by orders of magnitude to help find those that would be reasonable for the migration process based on literature [7] [4].

Changing h_{max}

We use the MATLAB PDE toolbox to solve our diffusion equation, which uses the finite element method to approximate a numerical solution. One of the parameter options is 'h_{max},' which is the largest size we will allow for an element. A larger h_{max} means fewer elements, a coarser approximation, and faster computation.

When simulating the migration, we used the default h_{max} of 15.22. For convenience, when testing for these experiments, we used an h_{max} of 100, since that value worked most reliably across different machines. We tested the interpolated concentration and magnitude of the x component of the gradient at various points along the central chamber for solutions derived by meshing with different values of h_{max}. Although the values do change depending on the fineness of the mesh (Tables 4 and 5), we decided that the differences were insignificant since changing h_{max} by factors as high as 15 did not result in much more than a 10% change in the gradient or concentration values. Therefore, we chose other parameters to change when running other tests.

We also tested diffusion with various values for h_{max} and recorded the total number of nodes and the time for diffusion to run in each case (Table 6). We found that there was not a linear relationship between the increase in h_{max} and the number of total nodes in our diffusion model. We also concluded that the number of total nodes was not proportional to the time needed to run the diffusion. In fact, we found that the models with a larger number of nodes ran slower, meaning they ran with a lower node per second rate than those trails with lower total node counts.

h_{max}	$x = 100\,\mu m$	$x = 200\,\mu m$	$x = 300\,\mu m$	$x = 400\,\mu m$
10	5001	12527	31101	57230
15.22 (Default)	5001	12505	31047	57117
25	5061	12617	31233	57347
50	5122	12718	31306	57683
75	5206	12884	31757	58230
100	5456	13481	32608	59179
125	5459	13336	32635	60285
150	5335	13287	32528	60466

Table 4: Concentration (pM in the Egg Chamber with Varying h_{max} Values)

h_{max}	$x = 100\,\mu m$	$x = 200\,\mu m$	$x = 300\,\mu m$	$x = 400\,\mu m$
10	33.2579	131.6509	171.1896	161.3633
15.22 (Default)	31.8730	130.8314	170.8976	163.7170
25	31.8606	131.0277	176.9875	164.3742
50	32.1271	130.9679	179.8976	166.9111
75	33.3266	134.3933	182.4712	160.6950
100	35.5692	132.2848	176.7885	158.7610
125	32.3669	134.9576	178.5561	159.0558
150	35.2204	130.8557	185.0690	152.3882

Table 5: x Component of the Gradient ($\mathrm{pM}\,\mu m^{-1}$) with Varying h_{max} Values

h_{max}	Number of nodes	Time (s)
10	91716	767.75
15.22 (Default)	31407	113.77
25	20367	63.526
50	10097	21.703
75	6499	12.477
100	5167	8.779
125	4643	8.221
150	4251	7.707

Table 6: Number of Nodes and Running Times After Changing h_{max}

Time for Chemoattractants to Diffuse Across Entire Egg Chamber

It is understood that a chemoattractant triggers the migration of the polar and border cell cluster [1]. In particular, a gradient in the egg chamber is necessary for migration [1]. Therefore it is important, when considering diffusion, to know when the chemoattractant diffuses to a critical level at the anterior end of the egg chamber. For this reason, we chose the farthest point from the source of secretion to test for a substantial amount of chemoattractant concentration. The point we chose to test was $(20\,\mu m, 146.25\,\mu m, 146.25\,\mu m)$, located on the anterior end of our egg chamber central in the y and z directions. Before testing how long it would take for the chemoattractant to reach the anterior side of the egg chamber, we had to determine what chemoattractant concentration would be sufficient for the anterior side in order for us to consider that the chemoattractant had "reached the other side". For this we chose the arbitrary number of 1 pM as a baseline for considering what has substantial chemoattractant concentration (these results are listed in table 7).

We first tested the time across using various D values ranging from $0.01\,\mu m^2\,s^{-1}$ to $100\,\mu m^2\,s^{-1}$ on a logarithmic scale, also listed in Table 7. With the values of $0.01\,\mu m^2\,s^{-1}$ and $0.1\,\mu m^2\,s^{-1}$, the diffusion of the chemoattractant did not reach the end of the egg chamber after five hours, leading us to believe that D needs to be greater than $0.1\,\mu m^2\,s^{-1}$. We also observed that as D increases, the amount of time it would take to reach the end of the egg chamber decreases.

Different values of k were also tested to find their impact on the time to the 1 pM mark at the anterior. The parameter k is the uptake of chemoattractant in the extracellular space. Uptake is the rate at which chemoattractant breaks down. The values tested were $1 \times 10^{-2}\,s^{-1}$ to $1 \times 10^{-6}\,s^{-1}$ on a logarithmic scale. With k values of $1 \times 10^{-2}\,s^{-1}$ and $1 \times 10^{-3}\,s^{-1}$, as seen in Figure 7, the time for the chemoattractant to diffuse across the egg chamber surpassed the five hour mark. This suggests that k values of $1 \times 10^{-2}\,s^{-1}$ and $1 \times 10^{-3}\,s^{-1}$ may be too high. We also saw that as k decreased, the time for the complete diffusion decreased by only a small fraction. This led us to believe that after a certain value, the change in k does not have a large effect on the time it takes for the chemoattractant to diffuse to the anterior end.

The next parameter ϕ is the uptake of chemoattractant into the nurse cells. Values from $1 \times 10^{-2}\,\mu m\,s^{-1}$ to $1 \times 10^{-5}\,\mu m\,s^{-1}$ were tested on a logarithmic scale. We found that for a value of $\phi = 0.1\,\mu m\,s^{-1}$, the chemoattractant did not reach 1 pM at the anterior of the egg chamber in under five hours, and this suggests that ϕ should be less than $0.1\,\mu m\,s^{-1}$. Similar to our results for k, other values of ϕ caused minimal change in the time values; there was only a slight decrease in the time taken for the chemoattractants to diffuse across the egg chamber when ϕ was decreased. Therefore, changing ϕ after $0.1\,\mu m\,s^{-1}$ does not have much of an impact on the time it takes for the chemoattractants to diffuse to the end of the egg chamber.

The secretion constant σ is the amount of secreted chemoattractant per unit of space in a given time. The values of σ that we tested ranged from $1\,pM\,\mu m\,s^{-1}$ to $10\,000\,pM\,\mu m\,s^{-1}$ on a logarithmic scale. We found that the higher values of σ needed less time for the point in the anterior of the egg chamber to reach a 1 pM concentration as would be expected. Changing this variable resulted in the largest range of times for the chemoattractant to reach the end, as can be seen in Table 7. However, it is important to note that σ did not make the chemoattractant diffuse faster but rather amplified the concentration of the chemoattractant that was being diffused so that it rose above the 1 pM level in fewer seconds; σ does not change the rate of diffusion but rather it changes the magnitude of the diffused chemoattractant.

For an internal view of the secretion of chemoattractant at the point at which it reached the apical end of the egg chamber, see Figure 4.1, which displays the extracellular concentration of chemoattractant in the egg chamber. That figure shows the chemoattractant being secreted from the full face of the oocyte as well as the epithelium where $x \geq 300\,\mu m$. The diffusion parameters are $D = 1\,\mu m^2\,s^{-1}$, $k = 10 \times 10^{-5}\,s^{-1}$, $\phi = 0\,\mu m\,s^{-1}$, and $\sigma = 100\,pM\,\mu m\,s^{-1}$, and the time step shown, which is when the chemoattractant officially reaches the apical end based on our baseline, is after 203 seconds.

We experimented with maintaining the same parameters except for doubling the value of σ. On the graph with the doubled value of σ, we also doubled the color scale, making the graphs the exact same. This shows that the diffusion did not go any faster with a change in σ, but instead that the concentration at each point in the egg chamber doubled. This demonstrated that a change in σ is directly proportional to the change in the concentration level at each point. However, this is expected due to the linearity of our diffusion reaction model.

D value ($\mu m^2\,s^{-1}$)	10^{-2}	10^{-1}	10^{0}	10^{1}	10^{2}
Time across (h)	> 5	> 5	1.015	0.145	0.130

k value (s^{-1})	10^{-6}	10^{-5}	10^{-4}	10^{-3}	10^{-2}
Time across (h)	1.010	1.015	1.055	> 5	> 5

ϕ value ($\mu m\,s^{-1}$)	10^{-5}	10^{-4}	10^{-3}	10^{-2}	10^{-1}
Time across (h)	1.015	1.015	1.040	1.385	> 5

σ value ($pM\,\mu m\,s^{-1}$)	10^{0}	10^{1}	10^{2}	10^{3}	10^{4}
Time across (h)	2.055	1.390	1.015	0.765	0.580

Table 7: Time for Chemoattractant to Cross Egg Chamber ($k = 10 \times 10^{-5}\,s^{-1}$)

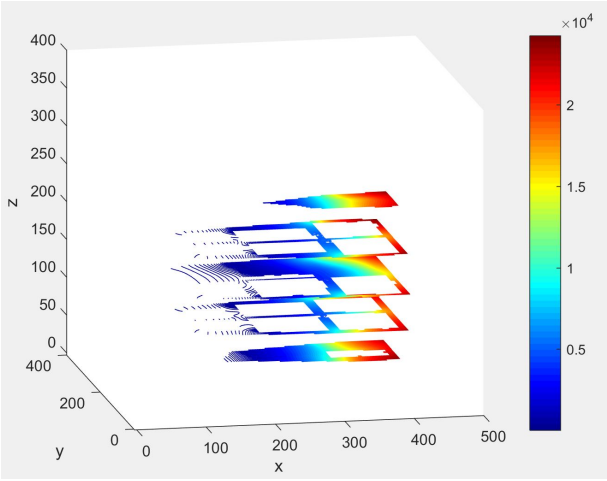

Figure 3: Extracellular View of Chemoattractant Reaches 1 pM at Anterior End ($k = 10 \times 10^{-5}\,s^{-1}$)

D value ($\mu m^2\, s^{-1}$)	10^{-2}	10^{-1}	10^{0}	10^{1}	10^{2}
Time (h)	2.97	3.13	2.92	3.24	3.29

k value (s^{-1})	10^{-6}	10^{-5}	10^{-4}	10^{-3}	10^{-2}
Time (h)	> 5	4.87	2.92	0.84	0.16

ϕ value ($\mu m\, s^{-1}$)	10^{-5}	10^{-4}	10^{-3}	10^{-2}	10^{-1}
Time (hrs)	2.91	2.85	2.38	1.15	0.41

σ value ($pM\, \mu m\, s^{-1}$)	10^{0}	10^{1}	10^{2}	10^{3}	10^{4}
Time (h)	2.92	2.92	2.92	2.92	2.92

Table 8: Time for Egg Chamber's Concentration to Reach a Steady State

D value ($\mu m^2\, s^{-1}$)	10^{-2}	10^{-1}	10^{0}	10^{1}	10^{2}
Time (h)	0.33	0.77	0.30	0.12	0.13

k value (s^{-1})	10^{-6}	10^{-5}	10^{-4}	10^{-3}	10^{-2}
Time (h)	0.30	0.30	0.30	0.39	0.12

ϕ value ($\mu m\, s^{-1}$)	10^{-5}	10^{-4}	10^{-3}	10^{-2}	10^{-1}
Time (h)	0.30	0.30	0.30	0.30	0.30

σ value ($pM\, \mu m\, s^{-1}$)	10^{0}	10^{1}	10^{2}	10^{3}	10^{4}
Time (h)	0.21	0.27	0.30	0.30	0.30

Cutoff value	10^{-2}	10^{-1}	10^{0}	10^{1}	10^{2}
Time (h)	4.26	1.31	0.60	0.18	0.02

Table 9: Time for Gradient's Direction to Reach a Steady State

4.2 Steady State of Diffusion

A steady state in diffusion is when the concentration of chemoattractant at each point reaches a level where it will consistently remain. To define our rate of change, we find a vector of the concentration at every element at a particular time step, then subtract the same vector for the previous time step, and take the Euclidean norm. When this value goes below a certain cutoff, we decide that the diffusion has reached a steady state. We estimated a cutoff of .0008 to be reasonable (Table 8).

In our current model, when calculating the migratory force, we do not consider the value of concentration nor the magnitude of the gradient. The only thing that we consider is the direction of the gradient. Therefore, it is useful to know when the direction of the gradient reaches a steady state.

To calculate the direction of the gradient, we normalized it. To find out how much a gradient in the x, y, or z direction has changed since the previous time step, we took the Euclidean norm of the difference of each component between the two time steps. The gradients were collected for 1000 time steps. Then, we add together the norm of the differences of all three spatial directions. When this value went below 3, that time step is determined as the directional steady state. The cutoff of 3 was qualitatively chosen, but considering that these simulations included around 5000 elements, it would indicate a very small change. For example, if the normalized derivative in each direction changed by about .01 at a time step, then this would give a value of 0.71. As with the concentration, the measure of changing gradient direction decreases over time, meaning the direction of the gradient becomes more stable (Table 9).

The values of ϕ and σ have little impact on the time to a steady state. The values of D and k affect it in non-obvious ways. With our definition of the steady state of the concentration and

$\phi = 10^{-5}$ $k = 10^{-5}$	Oocyte and Epithelium $\geq 200\,\mu m$	Oocyte and Epithelium $\geq 250\,\mu m$	Oocyte and Epithelium $\geq 300\,\mu m$	Oocyte and Epithelium $\geq 350\,\mu m$	Just Oocyte
$\sigma = 10$	4411.8	3646.3	2901.3	2042.2	959.85
$\sigma = 15$	6617.7	5469.4	4352.0	3063.2	1439.8
$\sigma = 30$	13235	10939	8703.9	6126.5	2879.5
$\sigma = 45$	19853	16408	13056	9189.7	4319.3
$\sigma = 60$	26471	21878	17408	12253	5759.1
$\phi = 10^{-4}$ $k = 10^{-4}$	Oocyte and Epithelium $\geq 200\,\mu m$	Oocyte and Epithelium $\geq 250\,\mu m$	Oocyte and Epithelium $\geq 300\,\mu m$	Oocyte and Epithelium $\geq 350\,\mu m$	Just Oocyte
$\sigma = 10$	2142.0	1781.3	1428.6	1013.2	478.24
$\sigma = 15$	3212.9	2672.1	2143.0	1519.9	717.37
$\sigma = 30$	6426.0	5344.2	4285.8	3039.8	1434.7
$\sigma = 45$	9638.9	8015.7	6428.9	4559.7	2152.0
$\sigma = 60$	12852	10688	8571.8	6079.6	2869.4
$\sigma = 75$	16065	13361	10715	7599.6	3586.8
$\sigma = 90$	19278	16033	12857	9119.3	4304.8
$\sigma = 95$	20349	16923	13571	9626.1	4543.3

Table 10: Average Concentration of Chemoattractant Based on Location and Quantity of Secretion

of the directional gradient, the directional gradient comes to a steady state much quicker in all scenarios. This makes sense because even with a changing concentration, the direction can already be established.

Average Amount of Chemoattractant in the Egg Chamber

We considered that the epithelium cells with the surface of the oocyte may be secreting the chemoattractant, so we experimented in changing how changing the amount of epithelial cells secreting and the total amount of chemoattractant secreted would affect the level of concentration in the egg chamber after 5 hours. We were searching for a combination that would produce an average chemoattractant concentration of approximately 4500 pM, the value given to us as a realistic and experimentally-verified amount. In this way, we changed the amount of epithelial cells that were secreting the chemoattractant by altering which locations of the epithelium of the egg chamber were actively secreting during certain trials. Considering that the coordinates of the egg chamber in the x direction go from 0 µm to 409.5 µm, we used epithelium locations including the oocyte and starting at 200 µm, 250 µm, 300 µm, 350 µm, and just the oocyte (at 409.5 µm). Then, for each of these chosen active areas, we changed the value of σ, the amount of chemoattractant entering the egg chamber, to determine the average chemoattractant concentration in the egg chamber after 5 hours of that specified location secreting that specified concentration (Table 10).

Many conclusions could be drawn from such a test. As expected, keeping the area of secreting epithelium cells the same, as we increased σ, the concentration in the egg chamber increased proportionally. Keeping σ the same and increasing the amount of epithelial cells secreting also caused the final average chemoattractant concentration in the egg chamber to increase.

We then tested the same σ values and locations of secretion with two different values of k and ϕ, the extracellular degradation and nurse cell uptake of chemoattractant respectively. When we increased k and ϕ by a factor of 10, changing them from $10 \times 10^{-5}\,s^{-1}$ to $10 \times 10^{-4}\,s^{-1}$ and from $10 \times 10^{-5}\,\mu m\,s^{-1}$ to $10 \times 10^{-4}\,\mu m\,s^{-1}$ respectively, we observed the concentration average decrease for corresponding combinations of secretion location and σ value. This is logical because more of the chemoattractant is lost by the nurse cells. However, it is interesting to note that it cuts the average concentration almost exactly in half. Looking at Figure 4, each pair of adjacent lines, starting with any tall one and looking at the shorter one directly to its right, shows that increasing k and ϕ by a factor of 10 and doubling σ, but maintaining all other parameters will cause the average concentration to be cut in half.

Therefore, when thinking about the value of σ needed to produce an average concentration

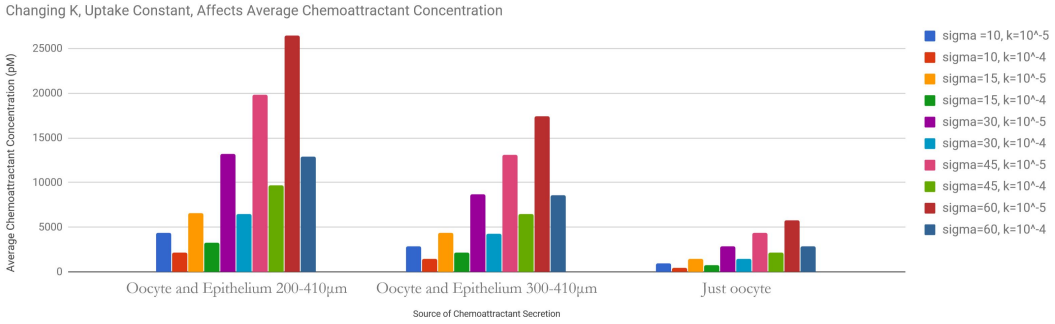

Figure 4: The Relationship Between Pairs of Sources and Strengths of Secretion

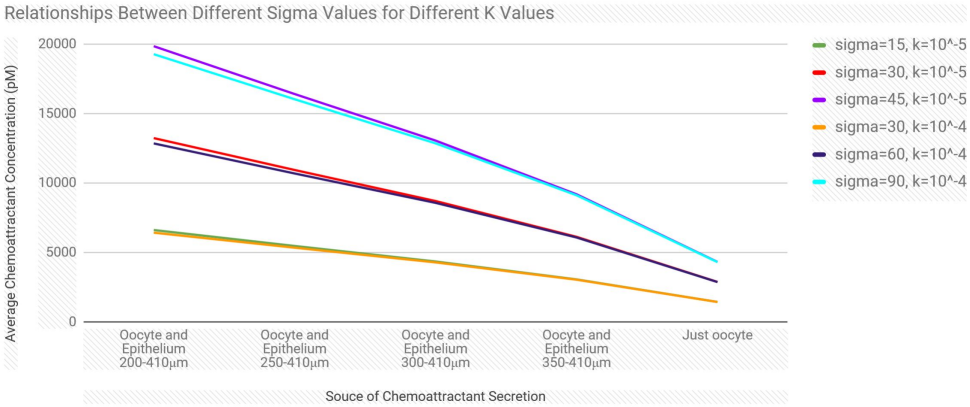

Figure 5: Average Concentration Values for Changing σ and k

level of approximately 4500 pM after 5 hours of diffusion, maintaining the same secretion location and increasing k by a factor of 10 will necessitate doubling the value of σ in order to reach this realistic chemoattractant value. So for a measured average concentration of chemoattractant these tables can be used to find appropriate secretion values.

Difference in Gradients at Various Points in Egg Chamber

A gradient of chemoattractants is understood to be necessary for cell migration, but the way the cluster takes cues from the gradient is unknown [1]. In particular, we investigate the extent that the cluster uses the magnitude of the gradient to cause and direct movement. One possibility we investigated is that the cluster responds linearly to the magnitude of the gradient. To determine if this is plausible, we tested the magnitude of the x component of the gradient along with the chemoattractant concentration at points near the anterior and posterior ends of the egg chamber. We then used a point at the posterior end and a point at the anterior end (Figure 4.2) and found the ratio of the gradient and concentration (Tables 11 and 12).

When k and ϕ had higher values, such as $0.01\,\mu\mathrm{m\,s^{-1}}$ and $0.01\,\mathrm{s^{-1}}$ or $0.1\,\mu\mathrm{m\,s^{-1}}$ and $0.1\,\mathrm{s^{-1}}$, there was a greater difference in concentration because more chemoattractant would deteriorate before reaching the end. When $k = 10 \times 10^{-2}\,\mathrm{s^{-1}}$, there was too little concentration at the anterior to give a reliable value. For certain values of ϕ and when half of the epithelium was secreting, the x component of the gradient actually pointed backwards at the anterior end at the end of diffusion, and this could cause problems during migration, pointing the migratory force away from the oocyte. The concentration decreased everywhere, but less so near the oocyte. A high D, like $1000\,\mu\mathrm{m^2\,s^{-1}}$, gave a concentration that was lower near the oocyte, but higher in the anterior because the chemoattractant was able to diffuse more freely. Changing σ causes no difference in the ratio of either concentration or gradient because it is only a scaling factor. Using a larger area of secretion makes the ratio decrease. In general, changing concentration ratios corresponded with changing gradient ratios.

No matter how we changed the parameters, every simulation resulted in gradients at opposite ends of the egg chamber whose value differed by at least one order of magnitude. We concluded that

D value ($\mu m^2\,s^{-1}$)	10^{-2}	10^{-1}	10^{0}	10^{1}	10^{2}
$x = 400\,\mu m$	4.33×10^{3}	8.01×10^{2}	1.33×10^{2}	1.69×10^{1}	1.76
$x = 20\,\mu m$	–	8.84×10^{-5}	1.73×10^{-2}	6.45×10^{-3}	7.63×10^{-4}
Ratio	–	9.06×10^{6}	7.71×10^{4}	2.62×10^{3}	2.31×10^{3}
k value (s^{-1})	10^{-6}	10^{-5}	10^{-4}	10^{-3}	10^{-2}
$x = 400\,\mu m$	1.62×10^{2}	1.59×10^{2}	1.33×10^{2}	8.18×10^{1}	4.42×10^{1}
$x = 20\,\mu m$	4.53×10^{-2}	4.12×10^{-2}	1.73×10^{-2}	1.49×10^{-4}	–
Ratio	3.58×10^{3}	3.85×10^{3}	7.71×10^{4}	5.48×10^{5}	–
ϕ value ($\mu m\,s^{-1}$)	10^{-5}	10^{-4}	10^{-3}	10^{-2}	10^{-1}
$x = 400\,\mu m$	1.33×10^{2}	1.34×10^{2}	1.41×10^{2}	1.26×10^{2}	9.58×10^{1}
$x = 20\,\mu m$	1.47×10^{-2}	-6.10×10^{-3}	-9.52×10^{-2}	-6.71×10^{-3}	9.59×10^{-6}
Ratio	9.04×10^{3}	-2.20×10^{4}	-1.48×10^{3}	-1.88×10^{4}	1.00×10^{7}
σ value ($\mu m\,s^{-1}$)	10^{0}	10^{1}	10^{2}	10^{3}	10^{4}
$x = 400\,\mu m$	1.33	1.33×10^{1}	1.33×10^{2}	1.33×10^{3}	1.33×10^{4}
$x = 20\,\mu m$	1.73×10^{-4}	1.73×10^{-3}	1.73×10^{-2}	1.73×10^{-1}	1.77
Ratio	7.71×10^{3}	7.71×10^{3}	7.71×10^{3}	7.71×10^{3}	7.71×10^{3}
Secretion Location	$\geq 200\,\mu m$	$\geq 250\,\mu m$	$\geq 300\,\mu m$	$\geq 350\,\mu m$	Just oocyte
$x = 400\,\mu m$	1.25×10^{2}	1.29×10^{2}	1.33×10^{2}	1.33×10^{2}	1.94×10^{1}
$x = 20\,\mu m$	-1.38×10^{-2}	2.34×10^{-2}	1.73×10^{-2}	1.33×10^{-2}	1.07×10^{-2}
Ratio	-9.11×10^{3}	5.51×10^{3}	7.71×10^{4}	9.98×10^{3}	1.81×10^{3}

Table 11: Ratio of x Component of Gradients ($pM\,\mu m^{-1}$) from Front to Back

the migratory force did not scale linearly to the magnitude of the gradient because real experiments show a relatively constant migration speed. It may be that there is a low saturation point where the force stops increasing linearly, the force is very nonlinearly related, or that the migratory force only depends on the direction of the gradient.

Results When Nurse Cells are Removed

An important question about cell migration is how the nurse cells interact with the diffusion of the chemoattractant. In our model, they either completely impede it, when $\phi = 0$, or uptake some level of chemoattractant when ϕ is nonzero. Our model leaves space (approximately 19.5 µm, the diameter of an IMC) between nurse cells for the chemoattractant to travel, but in reality, it can be inferred that the pathways could be narrower [5].

We also decided to consider what would happen to the established gradient if the chemoattractant could travel through the nurse cells or be absorbed by them as a part of the sink in the egg chamber. To get an idea of the effect of nurse cells blocking chemoattractant, we tested the concentration and x component of the chemoattractant at different points (at $x =$ 20 µm, 100 µm, 200 µm, 300 µm, and 400 µm) along the central corridor after a diffusion was done on both a geometry with nurse cells and one without them.

We found that the chemoattractant is more evenly dispersed without nurse cells (Table 13). There is a greater disparity between the concentration values at the posterior and apical ends of the egg chamber after the diffusion with the nurse cells; the same was found for the x component of the gradient. We can also observe that the nurse cells in the geometry cause the gradient to be stronger than what it would be had the nurse cells not been present (Table 14). We believe this is because that the nurse cells cause a barrier that prevents the chemoattractant from freely spreading itself farther away from the oocyte face. The results of this experiment imply that the narrower the domain in which the chemoattractant can disperse, the larger the range of the gradient and concentration in the egg chamber.

4.3 Migration

Table 15 displays the time the code took to run after various changes were made. After parallelizing the code for 16 processors, the code ran 13.8 times faster. After the approximations (the neighbor list and the constant gradient) were removed from the code, it still took less than twice as long, so the approximations were no longer necessary for the code to run in a reasonable amount of time.

D value ($\mu m^2\,s^{-1}$)	10^{-2}	10^{-1}	10^{0}	10^{1}	10^{2}
$x = 400\,\mu m$	3.50×10^{4}	3.43×10^{4}	3.22×10^{4}	1.86×10^{4}	1.52×10^{4}
$x = 20\,\mu m$	3.02×10^{-4}	7.90×10^{-3}	1.05×10^{3}	1.10×10^{4}	1.43×10^{4}
Ratio	1.16×10^{8}	4.34×10^{6}	3.05×10^{1}	1.69	1.06
k value (s^{-1})	10^{-6}	10^{-5}	10^{-4}	10^{-3}	10^{-2}
$x = 400\,\mu m$	6.36×10^{4}	5.92×10^{4}	3.22×10^{4}	4.17×10^{3}	4.18×10^{2}
$x = 20\,\mu m$	4.04×10^{3}	3.56×10^{3}	1.05×10^{3}	4.17×10^{1}	–
Ratio	1.57×10^{1}	1.66×10^{1}	3.05×10^{1}	1.00×10^{4}	–
ϕ value ($\mu m\,s^{-1}$)	10^{-5}	10^{-4}	10^{-3}	10^{-2}	10^{-1}
$x = 400\,\mu m$	3.21×10^{4}	3.11×10^{4}	2.36×10^{4}	7.08×10^{3}	1.80×10^{3}
$x = 20\,\mu m$	1.05×10^{3}	9.68×10^{2}	4.64×10^{2}	4.10	3.95×10^{-4}
Ratio	3.07×10^{1}	3.21×10^{1}	5.09×10^{1}	1.73×10^{3}	4.57×10^{6}
σ value ($\mu m\,s^{-1}$)	10^{0}	10^{1}	10^{2}	10^{3}	10^{4}
$x = 400\,\mu m$	3.22×10^{2}	3.22×10^{3}	3.22×10^{4}	3.22×10^{5}	3.22×10^{6}
$x = 20\,\mu m$	1.05×10^{1}	1.05×10^{2}	1.05×10^{3}	1.05×10^{4}	1.05×10^{5}
Ratio	3.05×10^{1}	3.05×10^{1}	3.05×10^{1}	3.05×10^{1}	3.05×10^{1}
Secretion Location	$\geq 200\,\mu m$	$\geq 250\,\mu m$	$\geq 300\,\mu m$	$\geq 350\,\mu m$	Just oocyte
$x = 400\,\mu m$	3.66×10^{4}	3.49×10^{4}	3.22×10^{4}	2.72×10^{4}	1.53×10^{4}
$x = 20\,\mu m$	3.75×10^{3}	1.94×10^{3}	1.05×10^{3}	5.31×10^{2}	8.48×10^{2}
Ratio	9.76	1.81×10^{1}	3.05×10^{1}	5.13×10^{1}	1.81×10^{1}

Table 12: Ratio of Concentrations (pM) from Front to Back

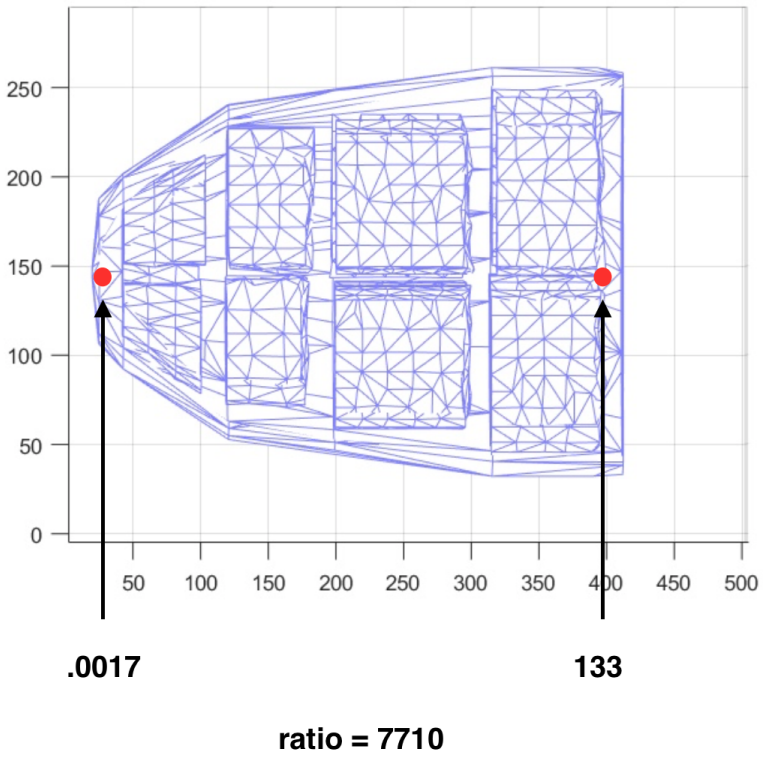

Figure 6: Two Points and Their Respective Gradients

x	Concentration With Nurse Cells	Concentration Without Nurse Cells
20	1055	960
100	1743	1394
200	5090	3590
300	14793	9239
400	32227	17449

Table 13: Concentrations With and Without Nurse Cells

x	x Gradient With Nurse Cells	x Gradient Without Nurse Cells
20	0.0173	0.0648
100	13.3547	10.3740
200	60.6631	35.6107
300	98.6105	73.7918
400	133.0300	95.4267

Table 14: x Components of the Gradient With and Without Nurse Cells

Code	Wall clock time (min)
Original code	152.10
Parallelized code	10.99
Parallelized code with no neighbors list	17.38
Parallelized code with diffusion calculation and no neighbors list	20.18

Table 15: Time to Run Code

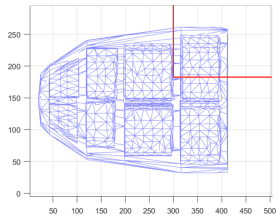

Figure 7: Secretion Location

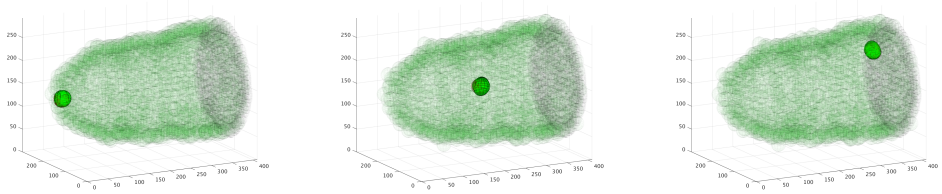

Figure 8: Cluster Migration (µm)

Vertical percentage of oocyte and epithelium secreting	Horizontal percentage of epithelium secreting	Average time of completed migrations (min)	Proportion of migrations completed
33%	0%	354.86	0.23
33%	25%	355.27	0.13
33%	50%	N/A	0
33%	75%	N/A	0
33%	100%	N/A	0
67%	0%	316.86	1
67%	25%	343.65	0.20
67%	50%	N/A	0
67%	75%	N/A	0
67%	100%	N/A	0
100%	0%	304.53	1
100%	25%	314.40	1
100%	50%	N/A	0
100%	75%	N/A	0
100%	100%	N/A	0

Table 16: Time of Migration

Vertical percentage of oocyte and epithelium secreting	Horizontal percentage of epithelium secreting	Average x (µm)	Average y (µm)	Average z (µm)
33%	0%	378.40	146.77	232.38
33%	25%	362.53	127.06	255.40
67%	0%	404.51	155.15	189.73
67%	25%	371.53	107.41	244.44
100%	0%	406.66	140.33	153.37
100%	25%	402.55	103.62	156.54

Table 17: Average Final Location Coordinates

Varying sources of chemoattractant were chosen to identify their effects on the migration of the cell cluster (Tables 16 through 20). To specify the locations where the chemoattractant was secreting, the xz-plane of the egg chamber was divided into four quadrants, and all of the epithelium and oocyte in the posterior dorsal quadrant secreted (0% horizontal means only the oocyte was secreting). As an example, if 25% of the horizontal distance and 33% of the vertical distance was secreting, the region of the egg chamber in the top right red box in Figure 7 would secrete chemoattractant. The sources were chosen to investigate how secreting from the epithelium affects the cell cluster migration and to test if secreting only from the top of the egg chamber could cause an accurate dorsal migration. For each source of chemoattractant, 30 simulations were run.

We investigated, for each source of chemoattractant, the proportion of migrations completed (those that reached the oocyte in less than 6 hours), and the average time of completed migrations (Table 16). Secreting from the epithelium makes the migration less reliable, with no migration with epithelium in the front 75% of the egg chamber secreting completing. In addition, secreting from only the dorsal side of the egg chamber also makes the migrations less reliable, with the smaller vertical regions of secretions resulting in a lower percentage of completed migrations. For the rest of the results, we considered only the 6 sources that resulted in a migration, even if the migration was inconsistent (specifically, those that secreted from just the oocyte or only 25% of the horizontal distance of the epithelium).

One example of a migration that we witnessed on our egg chamber model came from secreting the chemoattractant from the entire surface of the oocyte as well as those epithelial cells with x coordinates $\geq 300\,\mu m$. Three different shots from that 6 hour migration can be seen in Figure 8, taken at 22.5 minutes, 3 hours, and 6 hours.

To investigate the dorsal migration, we measured the average ending locations of the clusters (Table 17) and measured the average time it took for the cluster to leave the center of the yz-plane

Vertical percentage of oocyte and epithelium secreting	Horizontal percentage of epithelium secreting	Average time to leave center (min)	Proportion of migrations that left the center
33%	0%	73.47	1
33%	25%	29.49	1
66%	0%	117.24	1
66%	25%	38.10	1
100%	0%	316.69	0.83
100%	25%	158.88	1

Table 18: Time for Cluster to Leave Center

Vertical percentage of oocyte and epithelium secreting	Horizontal percentage of epithelium secreting	Sample standard deviation x (µm)	Sample standard deviation y (µm)	Sample standard deviation z (µm)
33%	0%	12.72	4.37	6.53
33%	25%	24.12	15.61	9.63
67%	0%	11.98	23.10	9.64
67%	25%	24.81	24.73	12.18
100%	0%	13.91	19.63	22.19
100%	25%	11.75	32.67	38.32

Table 19: Sample Standard Deviation of Final Locations

(defined as being more than 10% of the radius of the egg chamber away from the center) (Table 18). For reference, the oocyte is approximately a circle of radius 146.25 µm and the egg chamber is approximately a paraboloid of length 409.5 µm ending at the oocyte. Secreting from only the dorsal side of the egg chamber causes the cell cluster to migrate dorsally, as expected. However, it also causes the cell cluster to leave the center of the egg chamber earlier, which did not agree with what is observed biologically: a relatively straight migration to the oocyte followed by a dorsal migration at the oocyte. However, this is because the symmetry in our nurse cell geometry allows for a clear, open channel through which the cell cluster can gradually move dorsally along its horizontal journey to the oocyte surface instead of having that upward migration blocked by nurse cells until it first arrives at the oocyte surface. We attempted to rotate the geometry of the nurse cells to get rid of this symmetry and open channel, but the altered geometry was not feasible with the meshing protocol that we used at this time.

The last characteristic of the migration investigated was the standard deviation of the final location of the cluster, (Table 19). To calculate these values, we calculated the average location of the polar and border cells in the cluster for each trial, and then we calculated the standard deviation of these averages. Then, to test the claim that the standard deviations of the y and z coordinates are higher when chemoattractant is secreted from the epithelium as well, we assumed the null hypothesis that the standard deviations were the same, and obtained the p-values, that is, the probabilities that we obtained our results given that the standard deviations were the same (Table 20). For 100% and 33% of the oocyte secreting, the difference in both the the y and z standard deviations are significant at the $p = 0.05$ level, while the difference for 67% of the oocyte secreting is not. This result is reasonable, as secreting from the epithelium would cause the gradient

Vertical percentage of oocyte and epithelium secreting	y p-value	z p-value
33%	< 0.001	0.020
67%	0.358	0.107
100%	0.004	0.002

Table 20: p-Values for Standard Deviations

at off-center points in the egg chamber to point more towards the epithelium, compounding the effect of any minor deviations in the cell cluster's path. While there is not enough evidence to say this has an effect when only the top 67% of the oocyte is secreting, it is likely that this effect also exists there, and would be confirmed with more tests.

5 Conclusions

We found that the magnitude of the chemoattractant gradient varies greatly between ends of the egg chamber. Changing parameters mitigated this, but in all circumstances we investigated, the gradient on the posterior end is about 7700 times that of the anterior end. This caused us to use only the direction of the gradient to guide migration rather than the magnitude. Using a migratory force proportional to the gradient would make the force far too small at the beginning of migration and too large at the end for our simulation to be realistic to the observed in-vivo migrations. Larger nurse cells, which cause less space for diffusion, augments the disparity between the concentration and gradient values at opposite ends of the egg chamber, but even without any nurse cells, the difference between the concentration at each end and the gradient at each end persists in the five hour timespan of our diffusion model. In addition, we discovered that chemoattractant secretion from a larger range made the gap less extreme. Unless some parameters are more extreme than those for which we tested or the chemoattractant diffusion process takes longer than our allotted 5 hours, we conclude that the cluster migration mechanism is likely related to the gradient of the chemoattractant around it by either of three relationships. First, it could be a saturation function, meaning there would be a maximum migratory force, it could be sublinear, meaning it would grow less than proportionally, or it could solely depend on the direction of the gradient, like we model it in our simulation.

We were unable to produce biologically accurate dorsal migration in our simulation by just changing the source of chemoattractant alone. While this does not rule out the chemoattractant gradient being the cause of the dorsal migration (in particular, we were unable to test the migration model with a modified nurse cell geometry, which might change the chemoattractant gradient in a way that causes the dorsal migration), it does imply that there may exist some other unknown factors causing the dorsal migration. This is a potential avenue for further research, as incorporating the dorsal migration in the current model would make it more complete and help confirm that our current model is accurate.

We also found that chemoattractant secretion from the epithelium in addition to the oocyte causes less consistent migration, both by decreasing the percentage of successful migrations in 6 hours and by increasing the variability of the final location of the cluster after the 6 hour migration. Since the migration in the egg chamber is reliable with a small surface area of the epithelium secreting, it is implied that most of the epithelium likely does not secrete any chemoattractant.

Acknowledgments

These results were obtained as part of the REU Site: Interdisciplinary Program in High Performance Computing (hpcreu.umbc.edu) in the Department of Mathematics and Statistics at the University of Maryland, Baltimore County (UMBC) in Summer 2017. This program is funded by the National Science Foundation (NSF), the National Security Agency (NSA), and the Department of Defense (DOD), with additional support from UMBC, the Department of Mathematics and Statistics, the Center for Interdisciplinary Research and Consulting (CIRC), and the UMBC High Performance Computing Facility (HPCF). HPCF is supported by the U.S. National Science Foundation through the MRI program (grant nos. CNS–0821258 and CNS–1228778) and the SCREMS program (grant no. DMS–0821311), with additional substantial support from UMBC. Co-author Jessica Cooley was supported, in part, by the UMBC National Security Agency (NSA) Scholars Program through a contract with the NSA. Graduate assistant Morgan Strzegowski was supported by UMBC.

References

[1] Peter Duchek and Pernille Rørth. Guidance of cell migration by egf receptor signaling during drosophila oogenesis. *Science*, 291(5501):131–133, 2001.

[2] Peter Duchek, Kálmán Somogyi, Gáspár Jékely, Simone Beccari, and Pernille Rørth. Guidance of cell migration by the drosophila pdgf/vegf receptor. *Cell*, 107(1):17–26, 2001.

[3] UMBC HPCF. High performance computing facility - umbc, 2017.

[4] Shin Ishii Masataka Yamao, Honda Naoki. Multi-cellular logistics of collective cell migration. *PLoS One*, 6(12):e27950, 2011.

[5] Denise J. Montell, Wan Hee Yoon, and Michelle Starz-Gaiano. Group choreography: mechanisms orchestrating the collective movement of border cells. *Nature Reviews Molecular Cell Biology*, 2012.

[6] David Stonko, Dr. Michelle Starz-Gaiano, and Dr. Brad Peercy. Force-based biophysical model of border cell migration: Unraveling the mechanism of collective cell migration. An optional note, 2013.

[7] David P. Stonko, Lathiena Manning, Michelle Starz-Gaiano, and Bradford E. Peercy. A mathematical model of collective cell migration in a three-dimensional, heterogeneous environment. *PLoS One*, 10(4), 2015.